ELSEVIER

26 August 2002

Chemical Physics Letters 362 (2002) 483–490

CHEMICAL PHYSICS LETTERS

www.elsevier.com/locate/cplett

The intriguing near-ultraviolet photochemistry of H_2Te

J. Underwood, D. Chastaing [1], S. Lee, P. Boothe, T.C. Flood, C. Wittig *

Department of Chemistry, University of Southern California, Los Angeles, CA 90089-0482, USA

Received 17 May 2002; in final form 27 June 2002

Abstract

The ultraviolet absorption spectrum of H_2Te has a long wavelength tail that extends to 400 nm. Photodissociation at 355 nm yields $TeH(^2\Pi_{1/2})$ selectively relative to the $^2\Pi_{3/2}$ ground state; the transition moments for these channels lie in, and perpendicular to, the molecular plane, respectively. Vibrational structure in the region 380–400 nm is consistent with a shallow well in the adiabat leading to $^2\Pi_{1/2}$, akin to the one in HI leading to $I(^2P_{1/2})$. These effects have no counterparts with the light Group 6A dihydrides.

1. Introduction

Effects that are of a relativistic origin, i.e., arising from spin-orbit interaction and/or the increased mass that electrons acquire when they approach heavy nuclei, in general become progressively more important with increasing atomic number [1]. In the present context, this progression occurs upon going from oxygen to tellurium in the Group 6A hydrides: H_2O, H_2S, H_2Se, and H_2Te. A number of these effects are, or can be, manifest in studies of ultraviolet absorption and photodissociation, particularly at long wavelengths, where regions of curve crossings can be accessed via one-photon excitation processes. New vistas might emerge from such studies, and intuitions acquired from molecules that contain light atoms should be used with caution, if at all, when dealing with molecules that contain heavy atoms.

Though the H_2O molecule has been examined extensively [2,3], prior to the recent experiments of Plusquellic et al. [4] who measured the H/D branching ratio in the 193 nm photodissociation of HOD, and the corresponding theoretical study of Schröder et al. [5] relativistic effects in the lowest energy absorption system were believed to be unimportant. On the basis of these studies, however, the latter authors concluded that at long photodissociation wavelengths, such as 193 nm, the lowest triplet level, a^3B_1, plays a significant role. For example, they state: "*From all the experiences gained for this system in the last decade or so it should be clear that the surprisingly small measured values for the H/D branching ratio and the H_2O/D_2O cross-section ratio cannot be explained if exclusively excitation to the first excited singlet state is considered.*" In their work, the $a^3B_1 \leftarrow X^1A_1$ transition dipole moment could not be calculated

* Corresponding author. Fax: +1-213-746-4945.
E-mail address: wittig@usc.edu (C. Wittig).
[1] USC Women in Science and Engineering Postdoctoral Fellow.

0009-2614/02/$ - see front matter
PII: S0009-2614(02)01102-8

because spin–orbit interaction was not included in their Hamiltonian. A value was, however, inferred indirectly, and the transition dipole moment was found to be 4% as large as that of the strong $A^1B_1 \leftarrow X^1A_1$ transition. This is surprisingly large for a singlet–triplet transition in a small, light molecule. They also suggested that the a^3B_1 level might be important in the long wavelength photolysis of H_2S, accounting for the tail that extends to ~260 nm [6,7].

The H_2S molecule has been studied experimentally [6,7] and theoretically [8–10] – not as much as H_2O, but still very thoroughly – and the lowest energy absorption system is believed to be well understood [3,8,10]. No serious attention, however, has been directed toward the long wavelength tail. The ultraviolet absorption of H_2Se has also been studied [11]. No long wavelength tail has been noted; probably no one looked for it.

There are intriguing features of H_2Te that are not evident with its lighter counterparts. For example, in 1931 Goodeve and Stein [12] noted a long wavelength tail that extends all the way to 400 nm. No explanation of this feature has been given, or even attempted, in the intervening 70 years. It is almost certainly responsible for the light sensitivity of H_2Te, because the prominent feature that peaks ~ 250 nm lies well below the pyrex cutoff. Note that the absorption of a 400 nm photon by a ground state H_2Te molecule corresponds to an energy that is approximately 2200 cm^{-1} above the $TeH(^2\Pi_{3/2}) + H$ ground state product channel and approximately 1600 cm^{-1} *below* the $TeH(^2\Pi_{1/2}) + H$ product channel. Accessing repulsive potential curves from the ground vibrational level via a one-photon process at such small energies in excess of the large-r asymptotes is unheard of with lighter molecules. Note also that the $H_2 + Te$ product channel lies much lower in energy, as discussed below.

The long wavelength feature of H_2Te tempted us to consider the possibility that this molecule might be a source of tunable, fairly monoenergetic H atoms having modest translational energies. As discussed below, this in fact turns out to be the case.

The presence of pronounced relativistic effects in H_2Te invites detailed comparisons between experiment and theory, as has been done with HI [13–16], which is isoelectronic with H_2Te. Consequently, Sumathi and Balasubramanian [17] have calculated the energies of some product channels, a number of molecular properties and parameters for excited electronic states, and portions of their potential energy surfaces, albeit not the reaction paths for the different product channels. For example, they have predicted a bond dissociation energy of $D_0 = 65 \pm 3$ kcal/mol. No accurate experimental value was available at the time of this prediction. It will be shown below that their prediction proved to be accurate; the experimental value reported here is 65 ± 0.1 kcal/mol ($22{,}740 \pm 30$ cm^{-1}).

An important feature of this system is the large TeH spin–orbit splitting of 3815 cm^{-1} [18]. Curve crossings at large H–TeH distances can differ significantly from those of lighter systems, as has been seen with HI [15]. Because H_2Te has additional degrees of freedom (relative to HI), and spin-orbit interaction in TeH is smaller (by roughly a factor of two) than in the I atom, analogies with HI are valuable but should not be enlisted casually, as discussed below. Note that such curve crossings can influence reaction pathways much more than with light systems, even changing qualitatively the photoexcitation and exit channel dynamics.

2. Experimental methods and results

2.1. Sample preparation

Though H_2Te is the heaviest of the Group 6A hydrides that can be synthesized by using straightforward methods, its preparation and handling require great care. Reports of its sensitivities to light, impurities (especially water), surfaces, etc. are legion [19–22]; indeed, we have found that it can decompose at 77 K in the dark, yielding tellurium films and enough H_2 to rupture the glass vacuum line. It is also extremely toxic [21,22]. These obstacles probably account for the fact that H_2Te – which in principle is an attractive prototype for examining relativistic effects in a theoretically and

experimentally tractable molecule – has received little attention.

Several methods are available for the preparation of H_2Te [19,20]. The one we chose is to drop HCl onto ZnTe powder and collect and purify the resulting H_2Te vapor [19]. All chemicals (Alfa Aesar) were used as received and all glassware was dried overnight at 150 °C, assembled hot, and evacuated for approximately one hour before use.

In an N_2 glove box, 12 g of ZnTe was crushed with a mortar and pestle and added to a 100 ml round-bottom flask equipped with a Kontes joint sidearm. The flask was sealed and attached to a series of two U-tubes and a collection vessel, connected by greased ground-glass ball-and-socket joints with Teflon stopcocks on either side of each joint. The apparatus was connected to a vacuum line with Tygon tubing. A pressure-equalizing addition funnel was attached to the flask under N_2 pressure and the entire setup was evacuated for approximately 10 min. prior to beginning. Concentrated HCl (12.1 M) was bubbled with dry N_2 for ~ 10 min. and then added to the addition funnel by using 3 mm dia. Teflon tubing and N_2 pressure. Steel cannulae were avoided, as low levels of dissolved metal contaminants inhibited reaction.

The reaction was performed under a static N_2 atmosphere vented to a mercury bubbler. In a darkened room, portions of HCl (4 equivalents) were added to the ZnTe with vigorous stirring. Reaction progress was monitored by the rate of bubbling of the HCl/ZnTe solution, the progression of reaction color from red to gray, and the discoloration of the Teflon stopcocks by tellurium. The H_2Te gas thus produced passed through a trap (−15 °C dry ice/ethylene glycol cooled U-tube) before collection (−131 °C *n*-pentane/LN_2 slurry cooled U-tube).

After the reaction was complete, the reaction flask was sealed off and the U-tubes and collection flask were evacuated. LN_2 trapping of the vacuum line is essential. The collection vessel was cooled in a LN_2 bath and opened to the U-tubes as the pentane/LN_2 bath was removed, allowing H_2Te to diffuse into the vessel free from water and N_2. Yield was improved by back-transferring H_2Te trapped in the vacuum line LN_2 trap to the collection flask. Once collection was complete, the collection vessel was sealed and removed from the apparatus. Yields were variable. The H_2Te samples were transported to the building where the spectrophotometer traces were obtained and the photodissociation experiments discussed below were carried out. Samples decomposed rapidly. Clearly, H_2Te should be used shortly after its synthesis. It is likely that sample lifetimes can be increased by improved purification, particularly the removal of water.

2.2. Ultraviolet absorption spectra

As mentioned above, freshly prepared H_2Te samples were transported without delay to a Cary Series 50 spectrophotometer, where ultraviolet absorption spectra were recorded. Fig. 1a shows the main feature, consisting of a broad background with pronounced superimposed structure (peaked ~ 250 nm), as well as the long wavelength tail extending to ~ 400 nm. The tail region has been emphasized in Fig. 1b by using a higher sample concentration. This revealed – *to our surprise* – what appears to be a low frequency (~ 330 cm^{-1}) vibrational progression at the end of the long wavelength tail. Note that the shortest wavelength member of this progression appears at energies that are close to that of the $TeH\,^2\Pi_{1/2}$ excited spin–orbit channel. This was interpreted as a clue that the $^2\Pi_{1/2}$ level might play an important role in the long wavelength photochemistry.

2.3. Photodissociation experiments

The photodissociation of expansion cooled H_2Te was examined by using high-*n* Rydberg time-of-flight (HRTOF) spectroscopy. With cold (i.e., several K) parent molecules, measurements of H atom translational energy distributions (and conversion to center-of-mass (c.m.) translational energy distributions) yield the corresponding TeH internal energy distributions. The experimental arrangement is shown schematically in Fig. 2; it has been discussed in detail previously and will not be elaborated here [23]. The sensitivity of the arrangement shown in Fig. 2 is good and signal-to-noise ratio (S/N) has not been problematic. Fig. 3

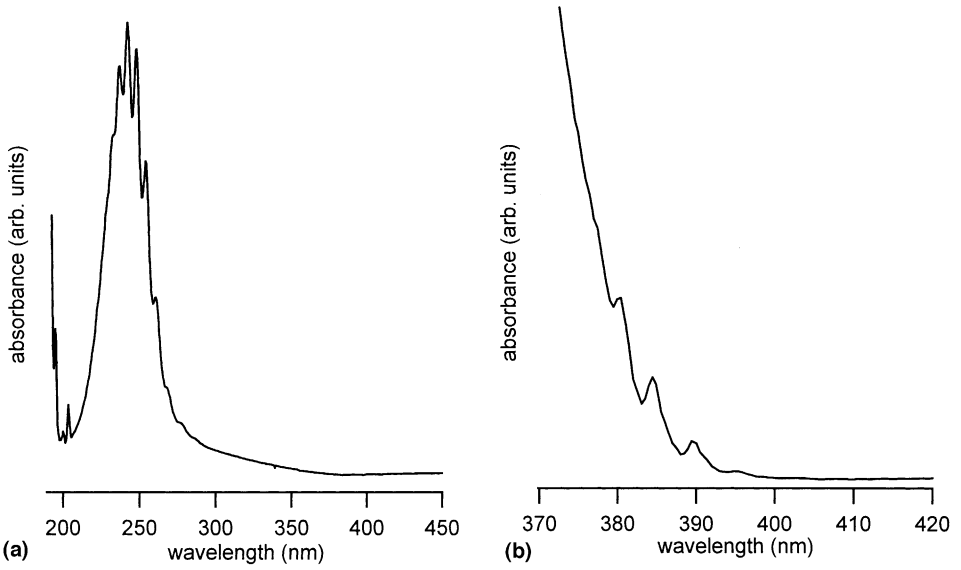

Fig. 1. (a) Absorption spectrum of H_2Te taken with a Cary Series 50 spectrophotometer. (b) A higher concentration sample emphasizes the long wavelength structure.

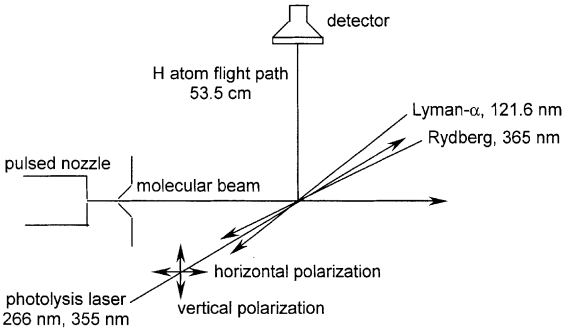

Fig. 2. Schematic of the HRTOF apparatus indicating the (polarized) photodissociation radiations (266 and 355 nm) and the radiations used to create high-n Rydberg H atoms (121.6 and 366 nm). The flight distance is 53.5 cm.

indicates the locations in the absorption spectra that are accessed by using 266 and 355 nm radiations. In each case, good S/N is achieved, e.g., because the small 355 nm absorption cross section is overcome easily by using high 355 nm fluences. The time-of-flight spectra were transformed to the c.m. translational energy distributions shown in Fig. 4.

The distributions shown in Fig. 4 yield a H—TeH bond dissociation energy of $D_0 = 22,$

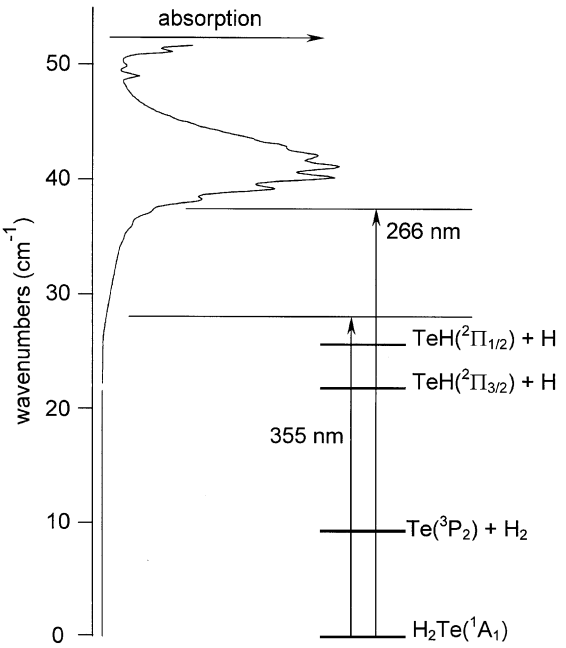

Fig. 3. H_2Te absorption spectrum and some product channel energies. Arrows indicate the photodissociation wavelengths used in this study. The H–TeH dissociation energy is from the present work, the $^2\Pi_{1/2}$–$^2\Pi_{3/2}$ splitting is from [18], and the H_2Te energy is obtained by assuming that D_0 for the TeH diatom is 22,740 cm^{-1}.

740 ± 30 cm^{-1}, which is, within the stated uncertainties, the same as the theoretical prediction of Sumathi and Balasubramanian [17]. The data also yield a $^2\Pi_{1/2}$–$^2\Pi_{3/2}$ separation of approximately 3820 cm^{-1}, in agreement with the accurate value of 3815.48 cm^{-1} obtained spectroscopically [18]. All of the observed TeH rotational and vibrational excitations are easily fitted by using available spectroscopic constants [18,24]. A high degree of spatial anisotropy is present, in which the $^2\Pi_{1/2}$ and $^2\Pi_{3/2}$ product channels derive mainly from transition dipole moments lying in, and perpendicular to, the H_2Te plane, respectively. This is consistent with rapid dissociation, ruling out significant participation by the X^1A_1 ground potential surface. Many lumpy features in the spectrum are due to photolysis of the TeH photoproduct. This aspect is of secondary importance here; it will be discussed later.

An important effect seen in Fig. 4a is selectivity toward the $^2\Pi_{1/2}$ state with 355 nm photodissociation. Of the tagged H atoms that reach the detector, $\sim 90\%$ correspond to TeH in the $^2\Pi_{1/2}$ state. A preliminary estimate of the branching is that $\sim$ two-thirds of the TeH is found in the $^2\Pi_{1/2}$ state; a detailed analysis will be presented later. A $^2\Pi_{1/2} - {}^2\Pi_{3/2}$ population inversion following broadband H_2Te photolysis has been noted in the early 1970's by Donovan and co-workers [25].

Referring to the 355 nm result shown in Fig. 4a, the c.m. translational energies associated with the $^2\Pi_{1/2}$ channel are distributed as per the TeH $v = 0$ rotational distribution. The $N = 0$ level corresponds to $E_{\text{trans}} = 1650$ cm^{-1}, and the average

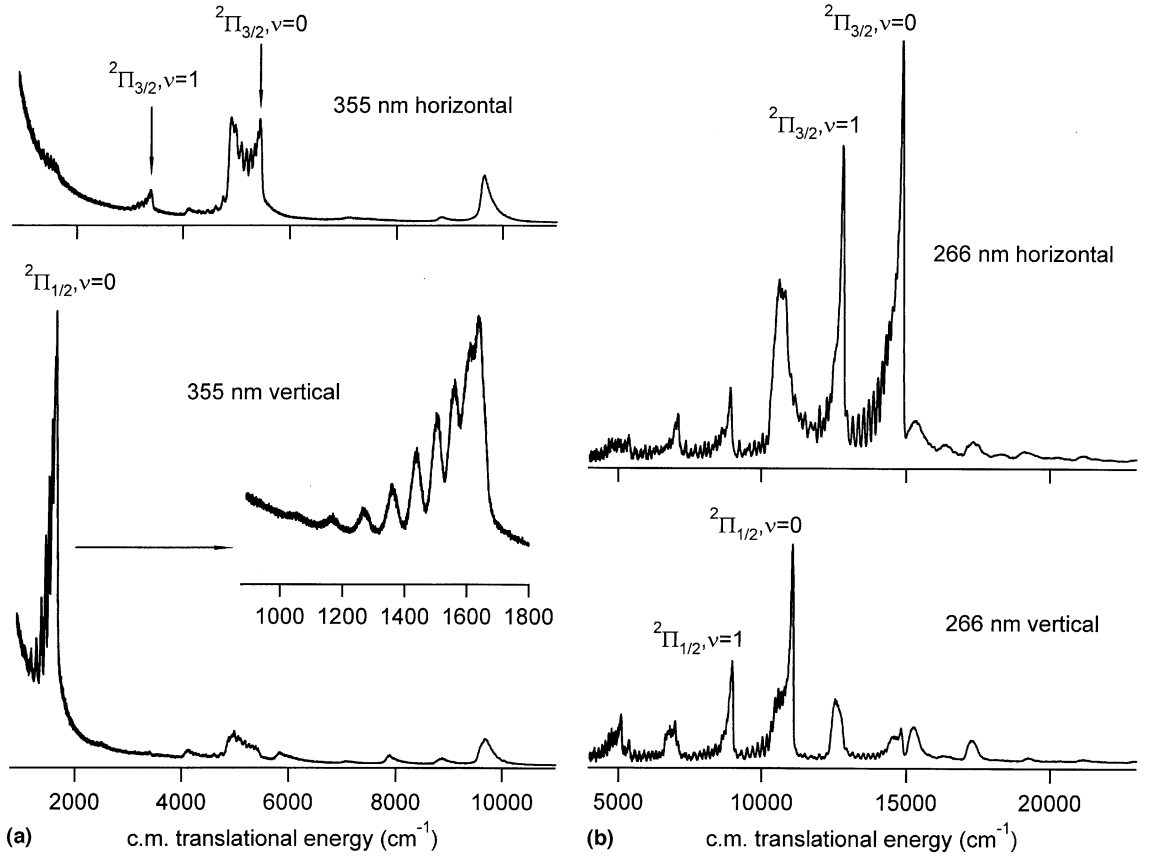

Fig. 4. Center-of-mass translational energy distributions for the photodissociation of H_2Te at (a) 355 nm and (b) 266 nm. Labels indicate TeH internal states.

rotational energy is ~ 60 cm^{-1}, corresponding to $\langle E_{\text{trans}} \rangle \simeq 1590$ cm^{-1}. Because of the TeH rotations, these H atoms are not monoenergetic. The spread is, however, significantly less than kT for room temperature samples. The $^2\Pi_{3/2}$ channel has essentially the same amount of rotational excitation and a small population of $v = 1$ (i.e., 1–2% of the total).

Fig. 4b shows the case of 266 nm photolysis. Many TeH internal states are populated and, as with 355 nm, there is significant secondary photolysis. Because it is almost certainly the case that several excited potential surfaces are involved, a discussion of these results will be deferred to a later publication.

3. Discussion and conclusions

As mentioned above, a high-level theoretical treatment of H_2Te has been carried out by Sumathi and Balasubramanian [17]. Properties of numerous electronic states were calculated, and a bond dissociation energy of $D_0 = 65 \pm 3$ kcal/mol was predicted. The D_0 value obtained in the present study (i.e., $22,740 \pm 30$ cm$^{-1} = 65 \pm 0.1$ kcal/mol) is in excellent agreement with the prediction. This augurs well for the possibility of reconciling the data presented herein with the theoretical model developed by Sumathi and Balasubramanian [17].

A qualitative comparison between H_2Te and its isoelectronic counterpart, HI, is appropriate. The latter has been studied extensively, and its lowest energy ultraviolet absorption, i.e., the A band, has been shown to be due to the superposition of three electronic transitions, i.e., from the $X^1\Sigma_{0^+}$ ground state to the $^3\Pi_1$, $^3\Pi_{0^+}$, and $^1\Pi_1$ states [13–16]. The recent paper by Alekseyev et al. [15] presents the results of high-level ab initio calculations of a number of molecular parameters, and agreement with the experimental data is excellent. In particular, accurate potential curves were calculated from the Franck–Condon region to products (Fig. 5), and absorption spectra, including $^2P_{1/2}/^2P_{3/2}$ branching ratios, were calculated for each of the participating curves. The $^2P_{1/2}$ channel is due to excitation of the $^3\Pi_{0^+}$ potential, which is repulsive

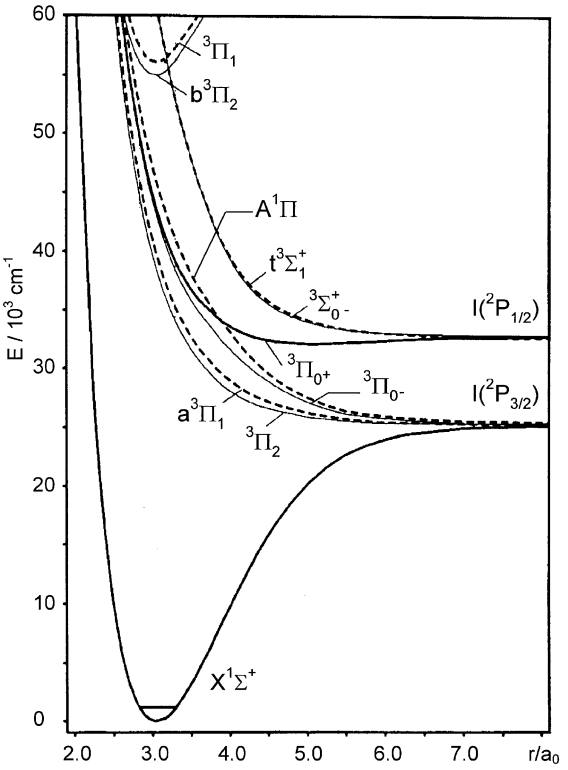

Fig. 5. Potential energy curves for the ground and low-lying excited electronic states of HI, adapted from Fig. 4 of [15].

except for a shallow well (having a depth of ~ 600 cm^{-1}) whose minimum is located at ~ 2.7 Å. It is predicted that this well can support two vibrational levels ($\omega_e \sim 370$ cm^{-1}), though the authors state that: "*...it should be difficult to observe these experimentally.*" Because of the relative locations of the $A^1\Pi$, $^3\Pi_{0^+}$, and $a^3\Pi_1$ curves, the $I(^2P_{1/2})$ quantum yield decreases monotonically for $h\nu > 40,000$ cm^{-1}, reaching zero at $32,000$ cm^{-1}.

With H_2Te, the curve that correlates adiabatically to $TeH(^2\Pi_{1/2})$ is expected to be similar to the $HI\,^3\Pi_{0^+}$ curve, but lower in energy by ~ 3790 cm^{-1}, i.e., roughly the difference between the $I(^2P_{1/2})$ energy (i.e., 7603 cm^{-1} relative to the $^2P_{3/2}$ ground state) and the $TeH(^2\Pi_{1/2})$ energy (i.e., 3815 cm^{-1} relative to the $^2\Pi_{3/2}$ ground state) [18]. This will result in a long wavelength tail and selectivity toward $TeH(^2\Pi_{1/2})$ over $TeH(^2\Pi_{3/2})$, as is observed in the 355 nm photodissociation result shown in Fig. 4. Furthermore, on the basis of this

analogy, it is predicted that the propensity toward $^2\Pi_{1/2}$ will be present throughout the long wavelength tail shown in Fig. 1.

The low frequency progression shown in Fig. 1b is believed to be the analog of the low frequency vibrations in the shallow well centered at ~ 2.7 Å noted in the theoretical study of the HI system [15]. The mean separation between peaks of approximately 330 cm^{-1}, which is close to the predicted $HI^3\Pi_{0^+}$ frequency (i.e., $\omega_e = 370$ cm^{-1}; no value of $\omega_e x_e$ was given), [15] as well as the precipitous fall-off toward 400 nm, are consistent with this interpretation. The linewidths seen in Fig. 1b may be due, at least in part, to parent rotation. It will be interesting to examine these features by using expansion-cooled samples. It is not a priori clear that the excitation of these features will result in H atom products, as the Te + H_2 channel lies at a much lower energy (Fig. 3).

A number of the interesting observations and molecular properties presented above are the consequence of strong spin–orbit interaction. For example, the shallow well of the $^3\Pi_{0^+}$ curve leading to $I(^2P_{1/2})$ is essentially van der Waals in character: because all electron multipole moments are zero for any level having $J = 1/2$, [26] the $^2P_{1/2}$ excited spin–orbit state is spherically symmetric and is attracted only weakly to the H atom. We expect there to be a direct counterpart in H_2Te, but not in H_2O or H_2S.

It is noteworthy that H atoms can be prepared having translational energies (E_{trans}) that are modest compared to those of other photolytic H atom sources. This E_{trans} regime is important for studies of reactive and inelastic processes that involve H atoms. For several decades, studies of "hot atom" reactions have been carried out by using H atoms having significantly larger E_{trans} values, typically > 1 eV, although 0.67 eV has been obtained by excluding the participation of the $I(^2P_{1/2})$ channel by using molecular beam techniques [27,28]. This regime, though providing valuable scientific information, is not characteristic of the many environments in which H atoms abound, e.g., combustion. In addition, the light hydrogen mass is known to inhibit the ability of systems to proceed along the lowest adiabatic pathways. A source of low energy, monoenergetic H atoms will be well received by scientists wishing to pursue such experimental studies.

The E_{trans} values can be varied as per the photolysis wavelength. Note that high photolysis fluences can be used because the long wavelengths are benign toward most light reactant species that may be present with the H_2Te H-atom precursor. In single-collision experiments, the high spatial anisotropy of the H-atom velocities can be used to select one or the other of the $^2\Pi_{1/2}$ and $^2\Pi_{3/2}$ channels, resulting in good translational energy resolution, as has been demonstrated with HI [27,28].

An interesting issue is the extent to which the trends observed at 355 nm can be extended to longer wavelengths. For example, at 365 nm, σ_{abs} is down by a factor of approximately 2, whereas the maximum E_{trans} value is 800 cm^{-1}. On the basis of the analogy with HI, we predict that the $^2\Pi_{1/2}$ channel will be accessed just as selectively as at 355 nm and the HTe rotational distribution will be slightly narrower. If these predictions are borne out, H_2Te will be an excellent photolysis source for tunable energy H atoms from several hundred cm^{-1} to several thousand cm^{-1}, provided that adequate care is taken in its preparation and handling.

Acknowledgements

This research was supported by the US Department of Energy, Office of Basic Energy Sciences, under grant number DE-FDG03-85ER1336. We acknowledge James Merritt for expert technical assistance, Krishnan Balasubramanian for scientific discussion, and Stephen Bradforth for the use of his group's ultraviolet spectrophotometer.

References

[1] K. Balasubramanian, Relativistic Effects in Chemistry, Parts A and B, Wiley, New York, 1997.
[2] V. Engel, V. Staemmler, R.L. Vander Wal, F.F. Crim, R.J. Sension, B. Hudson, P. Andresen, S. Hennig, K. Weide, R. Schinke, J. Phys. Chem. 96 (1992) 3201.
[3] R. Schinke, Photodissociation Dynamics, Cambridge University Press, Cambridge, 1993.

[4] D.F. Plusquellic, O. Votava, D.J. Nesbitt, J. Chem. Phys. 107 (1997) 6123.
[5] T. Schröder, R. Schinke, M. Ehara, K. Yamashita, J. Chem. Phys. 109 (1998) 6641.
[6] L.C. Lee, X. Wang, M. Suto, J. Chem. Phys. 86 (1987) 4353.
[7] C.Y.R. Wu, F.Z. Chen, J. Quantum Spectrosc. Radiat. Transfer 60 (1998) 17.
[8] B. Heumann, K. Weide, R. Düren, R. Schinke, J. Chem. Phys. 98 (1993) 5508.
[9] B. Heumann, R. Schinke, J. Chem. Phys. 101 (1994) 7488.
[10] D. Simah, B. Hartke, H.-J. Werner, J. Chem. Phys. 111 (1999) 4523.
[11] D.C. Dobson, F.C. James, I. Safarik, H.E. Gunning, O.P. Strausz, J. Phys. Chem. 79 (1975) 771.
[12] C.F. Goodeve, N.O. Stein, Trans. Far. Soc. 27 (1931) 393.
[13] D.A. Chapman, K. Balasubramanian, S.H. Lin, Chem. Phys. Lett. 118 (1985) 192.
[14] I. Levy, M. Shapiro, J. Chem. Phys. 89 (1988) 2900.
[15] A.B. Alekseyev, H.-P. Liebermann, D.B. Kokh, R.J. Buenker, J. Chem. Phys. 113 (2000) 6174.
[16] N. Balakrishnan, A.B. Alekseyev, R.J. Buenker, Chem. Phys. Lett. 341 (2001) 594.
[17] K. Sumathi, K. Balasubramanian, J. Chem. Phys. 92 (1990) 6604.
[18] D.A. Gillett, J.P. Towle, M. Islam, J.M. Brown, J. Mol. Spectrosc. 163 (1994) 459.
[19] L.M. Dennis, R.P. Anderson, J. Am. Chem. Soc. 36 (1914) 882.
[20] G. Brauer, Handbuch der Präparativen Anorganischen Chemie, Ferdinand Enke Verlag, Stuttgart, 1975.
[21] J.E. Macintyre, F.M. Daniel, V.M. Stirling (Eds.), Dictionary of Inorganic Compounds, vol. 3, Chapman and Hall, New York, 1992.
[22] R.B. King (Ed.), Encyclopedia of Inorganic Chemistry, vol. 8, Wiley, New York, 1994.
[23] J. Zhang, C.W. Riehn, M. Dulligan, C. Wittig, J. Chem. Phys. 104 (1996) 7027.
[24] E.H. Fink, K.D. Setzer, J. Mol. Spectrosc. 138 (1989) 19.
[25] D.J. Little, R.J. Donovan, R.J. Butcher, J. Photochem. 2 (1973) 451.
[26] R.N. Zare, Angular Momentum, Wiley, New York, 1988.
[27] L. Schnieder, K. Seekamp-Rahn, E. Wrede, K.H. Welge, J. Chem. Phys. 107 (1997) 6175.
[28] L. Bañares, F.J. Aoiz, V.J. Herrero, M.J. D'Mello, B. Niederjohann, K. Seekamp-Rahn, E. Wrede, L. Schnieder, J. Chem. Phys. 108 (1998) 6160.